Available online at www.sciencedirect.com
ScienceDirect
Remote Sensing of Environment 112 (2008) 107–117
Remote Sensing of Environment
www.elsevier.com/locate/rse

Forest vertical structure from GLAS: An evaluation using LVIS and SRTM data

G. Sun [a,*], K.J. Ranson [b], D.S. Kimes [b], J.B. Blair [b], K. Kovacs [c]

[a] Department of Geography University of Maryland, College Park, MD 20742 USA
[b] NASA's Goddard Space Flight Center, Greenbelt, MD, 20771, USA
[c] Science Systems and Applications, Inc. Lanham, MD, USA

Received 4 January 2006; received in revised form 29 August 2006; accepted 10 September 2006

Abstract

The Geoscience Laser Altimeter System (GLAS) on the Ice, Cloud and land Elevation Satellite (ICESat) is the first spaceborne lidar instrument for continuous global observation of the Earth. GLAS records a vertical profile of the returned laser energy from its footprint. To help understand the application of the data for forest spatial structure studies in our regional projects, an evaluation of the GLAS data was conducted using NASA's Laser Vegetation Imaging Sensor (LVIS) data in an area near NASA's Goddard Space Flight Center in Greenbelt, Maryland, USA. The tree height indices from airborne large-footprint lidars such as LVIS have been successfully used for estimation of forest structural parameters in many previous studies and served as truth in this study.

The location accuracy of the GLAS footprints was evaluated by matching the elevation profile from GLAS with the Shuttle Radar Topography Mission (SRTM) DEM. The results confirmed the location accuracy of the GLAS geolocation, and showed a high correlation between the height of the scattering phase center from SRTM and the top tree height from GLAS data. The comparisons between LVIS and GLAS data showed that the GLAS waveform is similar to the aggregation of the LVIS waveforms within the GLAS footprint, and the tree height indices derived from the GLAS and LVIS waveforms were highly correlated. The best correlations were found between the 75% waveform energy quartiles of LVIS and GLAS (r^2=0.82 for October 2003 GLAS data, and r^2=0.65 for June 2005 GLAS data). The correlations between the 50% waveform energy quartiles of LVIS and GLAS were also high (0.77 and 0.66 respectively). The comparisons of the top tree height and total length of waveform of the GLAS data acquired in fall of 2003 and early summer of 2005 showed a several meter bias. Because the GLAS footprints from these two orbits did not exactly overlap, several other factors may have caused this observed difference, including difference of forest structures, seasonal difference of canopy structures and errors in identifying the ground peak of waveforms.
© 2007 Elsevier Inc. All rights reserved.

Keywords: Forest structure; Lidar; GLAS; LVIS; SRTM; Height index; ICESat; Lidar waveform

1. Introduction

Vegetation spatial structure must be known to adequately monitor and model the carbon cycle and forest ecosystem dynamics. Most remote sensing systems, although providing images of the horizontal distribution of canopies (e.g., Landsat, MODIS), do not provide direct information on the vertical distribution of canopy elements. The lidar waveform signature from a large-footprint airborne lidar instrument, such as the Scanning Lidar Imager of Canopies by Echo Recovery (SLICER) (Harding et al., 2001) and the Laser Vegetation Imaging Sensor (LVIS) (Blair et al., 1999) have been successfully used to estimate tree heights and above-ground forest biomass (Drake et al., 2002; Dubayah & Drake, 2000; Lefsky et al., 1999a,b; Weishampel et al., 2000). Using LVIS data, Drake et al. (2003) found that lidar metrics, especially the height of median energy (HOME), were strongly correlated with mean stem diameter, basal area and above ground biomass (AGBM). Their studies found that these relationships differed between regions and that environmental factors have an important influence on these relationships. Hyde et al. (2005) found good agreement between field and lidar

* Corresponding author.
E-mail address: guoqing@ltpmail.gsfc.nasa.gov (G. Sun).

0034-4257/$ - see front matter © 2007 Elsevier Inc. All rights reserved.
doi:10.1016/j.rse.2006.09.036

measurements of height, cover, and biomass at the footprint level, and canopy height and biomass at the stand level. Differences between field and lidar measurements are mainly attributable to the spatial configuration of canopy elements. The studies using SLICER data by Lefsky et al. (2005a), though, found that the relationships between many stand structure indices and lidar measured canopy structure have generality at the regional scale. Lefsky et al. (2002) studied three biomes and found that a single equation explains major variance in above-ground biomass and shows no statistically significant bias in its predictions for any individual site. The differences in these studies may be due to the different data characteristics. Even though both SLICER and LVIS are large-footprint laser altimeter instruments, the footprint size, and vertical resolutions are different.

Lidar derived forest vertical parameters were used with an ecological model to model forest carbon storage and flux (Hurtt et al., 2004). In a study by Lefsky et al. (2005b), stand age mapped by iterative unsupervised classification of a multi-temporal sequence of Landsat TM images was cross-tabulated with estimates of stand height and aboveground biomass from lidar remote sensing to estimate the aboveground net primary production of wood. These studies showed the power of combining vegetation height information from lidar data with ecosystem models or other remote sensing data for estimates of carbon stocks and net carbon fluxes. Extending these analyses to larger scales will require the development of regional and global lidar data sets, and the continued development and application of height structured ecosystem models (Hurtt et al., 2004).

NASA and other agencies are interested in launching space-borne large footprint lidars (i.e., laser illuminated ground areas on the order of 10–100 m) in the near future (NASA, 2004). NASA tested the Shuttle Laser Altimeter-1 on Jan. 11–20, 1996, and Shuttle Laser Altimeter-2 on Aug. 7–18, 1997. NASA also launched the Mars Global Surveyor with the Mars Orbiter Laser Altimeter (MOLA) on Nov. 7, 1996, which started collecting data in early 1998. A European mission concept, Carbon 3-D, proposed to use a multi-angle imager in combination with a vegetation canopy lidar to extend the lidar-derived information to broader spatial coverage (Hese et al., 2005).

The Geoscience Laser Altimeter System (GLAS) instrument aboard the Ice, Cloud, and land Elevation (ICESat) satellite, launched on 12 January 2003. GLAS is the first lidar instrument designed for continuous global observation of the Earth (Zwally et al., 2002). Researchers have started using GLAS data for forest studies (Carabajal & Harding, 2005; Ranson et al., 2004a,b). In a recent paper by Lefsky et al. (2005c), combined ICESat GLAS waveforms and ancillary topography from SRTM were used to estimate maximum forest height in three ecosystems: tropical broadleaf forests in Brazil, temperate broadleaf forests in Tennessee, USA, and temperate needle leaf forests in Oregon, USA.

Measurements derived from lidar waveforms were used to characterize the canopy vertical structure. These measurements include the lowest and highest detectable returns (above a threshold noise level), and the heights within the canopy where 25, 50, 75 and 100% waveform energy were received (Blair et al., 1999). The vertical distribution of plant materials, along with the gap distribution, determines the proportion of energy scattered at a given height. The use of GLAS data for deriving accurate forest parameters for regional studies requires full understanding of their characteristics. The canopy height metrics derived from GLAS data will be evaluated in this study. The purpose of this study is to assess the data quality and information content of GLAS waveform and waveform-derived product GLA14. We will 1) assess the location accuracy of the GLAS footprint by comparing profiles of elevation measured by GLAS and SRTM; 2) compare the GLAS waveform with simulated waveform aggregated from all LVIS waveforms within the GLAS footprint; 3) evaluate the surface elevation and heights of waveform energy quartiles from GLAS with those derived from LVIS data; and 4) compare the tree height measured by two nearly repeated GLAS passes at different seasons to assess any temporal differences.

2. Study site and data

2.1. Study site

The test site (39°N, 76°50′W) is a forested area within the US Department of Agriculture's Beltsville Agricultural Research Center (BARC), north of the NASA's Goddad Space Flight Center (GSFC) in Maryland, USA. Fig. 1 shows a part of the study area using an image of top tree height from LVIS. The crosses on these figures are GLAS footprints. Two orbits from northwest to southeast, taken on Oct. 11, 2003 (white), and June 9, 2005 (blue), were analyzed in this paper. This area is very heterogeneous and is urban–suburban interface in the Baltimore–Washington corridor. The surface elevation ranges from

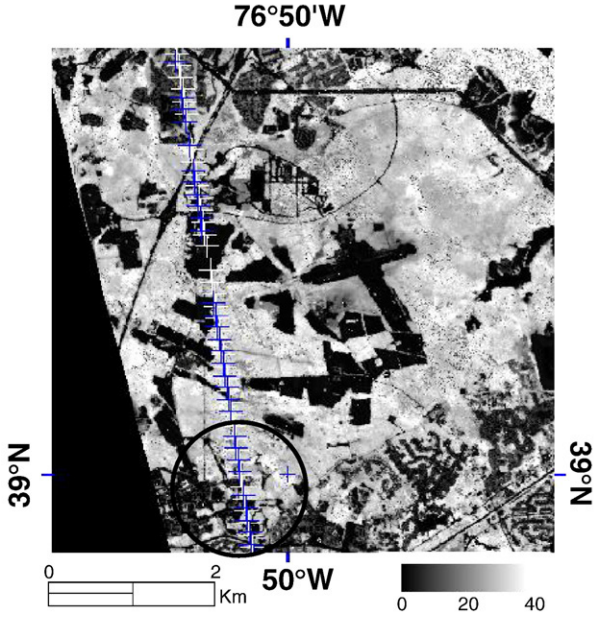

Fig. 1. LVIS height H100 image of a part of the study area. The cross symbols indicate the GLAS footprints of two near-repeat paths (white — Oct 11, 2003; blue— June 9, 2005). The black circle indicates the area where LVIS waveforms are available. (For interpretation of the references to colour in this figure legend, the reader is referred to the web version of this article.)

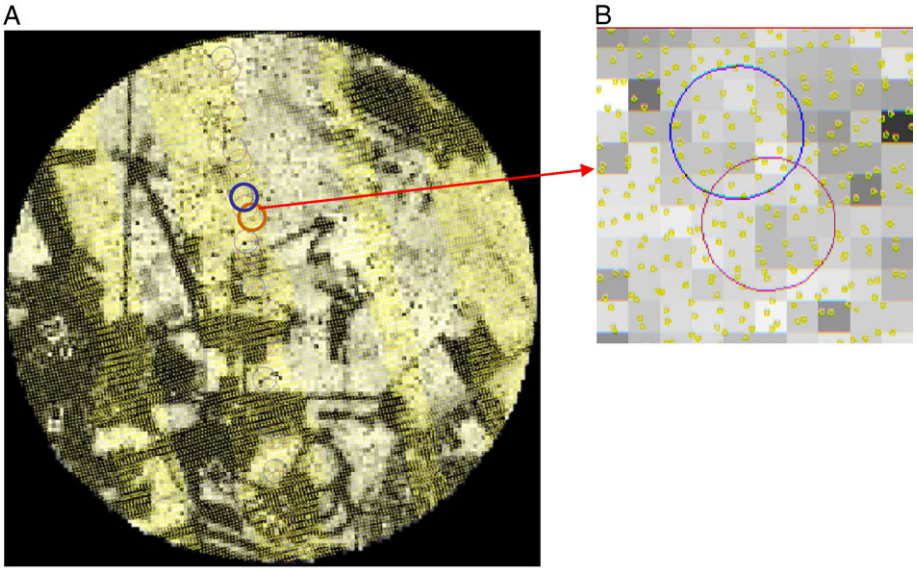

Fig. 2. A) LVIS (small yellow circles) and GLAS (maroon circle — Oct 11, 2003, blue circle — June 9, 2005) footprints overlay on gridded LVIS H100 image (15 m pixel). B) The circles represent ~60 m GLAS footprints. Each GLAS footprint encloses 30–40 LVIS shots. (For interpretation of the references to colour in this figure legend, the reader is referred to the web version of this article.)

near sea surface level to about 200 m from south to north. The forests in the area are mainly mixed forests dominated by pines (*Pinus virginia*) and oaks (*Quercus*spp.). The tallest trees reach a height of 40 m. Several GLAS footprints near GSFC were located using Global Position System (GPS). DBH (diameter at breast height) of all trees within a 30 m diameter circle were measured. The height of tall trees within the circle, and all dominant trees within a 60 m circle were also measured. These measurements were not used for quantitative analysis in this study due to limited points, but do provide a qualitative assessment of the GLAS data.

2.2. LVIS data

NASA's Laser Vegetation Imaging Sensor (LVIS) is an airborne laser altimeter system designed, developed and operated by the Laser Remote Sensing Laboratory at Goddard Space Flight Center. In 2003, LVIS obtained sub-canopy and canopy-top topography data as well as canopy vertical structure information for forested sites in New England and the US east coast in order to generate the most detailed forest structural data sets currently available for these regions. The LVIS data used in this study were acquired on August 14, 2003 (Blair et al., 2004) using footprint size of 10 m. LVIS Ground Elevation (lge) data were used, which include location (latitude/longitude), surface elevation, and the heights (relative to surface) where 25%, 50%, 75% and 100% of the waveform energy occur. LVIS geolocated waveform (lgw) data were also available within the black circle in Fig. 1. The height of 100% energy level (H100) of LVIS data for the study area was rasterized to 15 m × 15 m pixels using triangulation and linear interpolation in ENVI, and shown in Fig. 1. Fig. 2 shows the circular area with available LVIS waveforms. The smaller yellow circles represent locations of LVIS footprints and the larger circles are the GLAS footprints (see detail in the enlarged box — Fig. 2B).

A typical LVIS waveform of forest and the definition of these canopy structure measures are shown in Fig. 3. H25 is the 25% quartile height and is calculated by subtracting the ground elevation from the elevation at which 25% of the returned energy occurs. H100 is the canopy top height. These quartile heights are a relatively direct measure of the vertical profile of canopy components. In addition, waveform measures are a function of the complex and variable 3-D structure of canopy components and their spectral properties including the spectral properties of the ground/litter. The gap distribution within the canopy largely determines the amount of scattered energy at a given height that returns to the sensor.

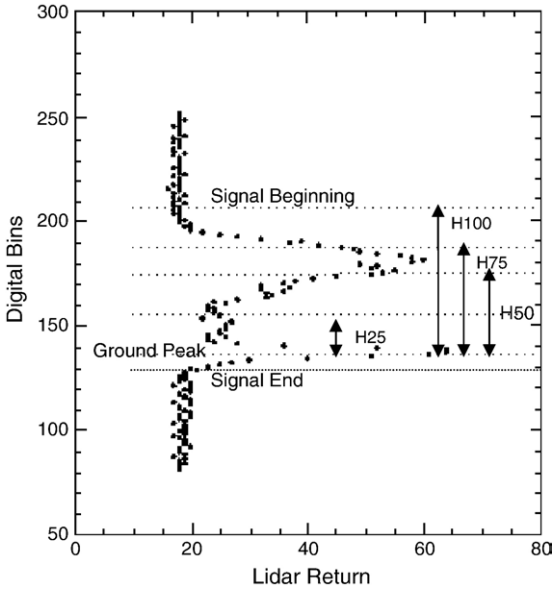

Fig. 3. A typical LVIS waveform with the definitions of energy quartiles.

2.3. GLAS data

GLAS carries three lasers. Laser 1 started firing on February 20, 2003 and failed on day 38. Because of the reduced lifetime of the laser system, the GLAS mission started to operate with a 91-day repeat orbit (with a 33 day sub-cycle). From early October to November 19, 2003, GLAS completed the first 33-day sub-cycle using laser 2 (L2A). Since then, three 33-day sub-cycle data sets have been acquired in Feb–March, May–June and October–November periods each year. The use of laser 3 was initiated in October, 2004 (L3A), and continued in February–March (L3B), May–June (L3C), October–November (L3D) in 2005, and Feb–March (L3E), May–June (L3F) in 2006. These 33-day sub-cycles are nearly repeat-passes of the October–November 2003 data (L2A), providing a capability for seasonal and inter-annual change monitoring. Based on transmitted power levels, the Oct–Nov, 2003 data are the best data acquired using the second laser on ICESat. The L3C data from the third laser in May–June, 2005 is a useful dataset for the spring and early summer seasons of the Northern Hemisphere.

GLAS uses the 1064-nm laser pulses and records the returned laser energy from an ellipsoidal footprint (the exp(−2) relative energy points along the edge). The footprint diameter is about 65 m, but its size and ellipticity have varied through the course of the mission (Abshire et al., 2005; Schutz et al., 2005). GLA01 products provide the waveforms for each laser shot, but only an estimated geolocation for all 40 shots acquired within 1 s. For the land surfaces, the waveform has 544 bins with a bin size of 1-ns or 15 cm. The bin size from bin 1 to 151 has been changed to 60 cm starting from acquisition L3A, so the total waveform length increased from 81.6 m to about 150 m. The product GLA14 (Land/Canopy Elevation) doesn't contain the waveform, but various parameters derived from the waveform. It is generated using algorithms and parameters which are appropriate for complex, multi-peaked waveforms (such as for rugged and/or vegetated landscapes). The GLAS waveforms were smoothed using filters, and the signal beginning and end were identified by a noise threshold. The smoothed waveform was initially fitted using many Gaussian peaks at different heights, and then the peaks were reduced to six by an iterative process (Harding & Carabajal, 2005; Zwally et al., 2002). GLAS14 data provides the surface elevation and the laser range offsets for the signal beginning and end, the location, amplitude, and width of the six Gaussian peaks. Fig. 4 shows a GLAS waveform from our study area with the Gaussian peaks (Hofton et al., 2000) and other parameters extracted from GLA14 data products. Assuming that the last peak near the ground is from surface reflection, the distance from the signal beginning and this ground peak is the top canopy height (referred to as H14). This works only for flat area, and requires significant return from ground surface. For cases with dense canopies, rough surfaces with slopes, the location of the ground peak becomes questionable.

The GLAS laser 2a had a range precision of <2.5 cm and a pointing determination accuracy better than 2″, corresponding to a horizontal geolocation error of 5.8 m (Abshire et al., 2005). According to Carabajal and Harding (2005), the horizontal geolocation error for Laser 3a, Release 22 was 2.4 m (mean) and 7.3 m (standard deviation). For this study, GLAS waveforms were extracted and processed to estimate the energy quartile heights similar to those from LVIS data products. The GLAS data used in this study were L2A (Release 26) acquired on Oct. 11, 2003, and L3C (Release 22) acquired on June 9, 2005 (Fig. 1). These two orbits are nearly repeat passes and are shown in Fig. 1 as the white and blue crosses. To verify the location accuracy of the GLAS footprint by comparing elevation measured by GLAS and SRTM requires a long profile of data, so that 600 GLAS footprint along track were used in the study. LVIS data didn't cover this long profile, so when comparing tree vertical parameters between GLAS and LVIS only those GLAS footprints covered by LVIS data (~200) were used. Since footprints from two orbits were not exactly repeated, only 40 footprints from each orbit with closest locations were used to compare the tree height measured from these two GLAS orbits.

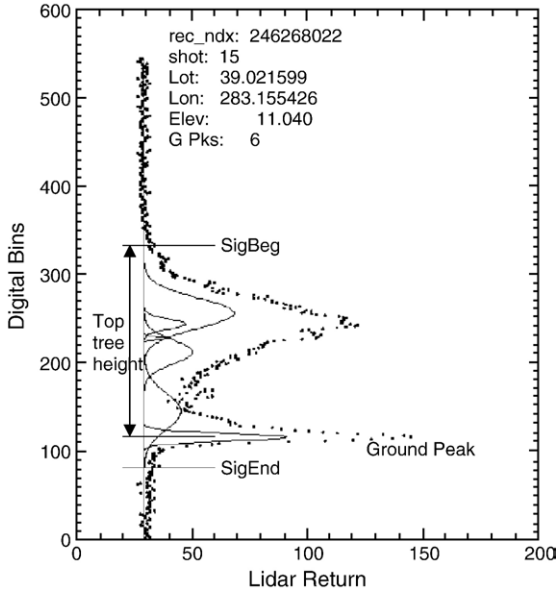

Fig. 4. A GLAS waveform in the study area: Dots — GLAS waveform data from GLA01, solid curves — Gaussian peaks used to fit the waveform from GLA14. Top tree height is the distance from signal beginning to the first Gaussian peak, i.e. the ground peak.

2.4. SRTM data

The Shuttle Radar Topography Mission (SRTM) was an international project sponsored by the National Imagery and Mapping Agency (NIMA)[1] and NASA (van Zyl, 2001). SRTM consisted of a fixed-baseline interferometric C-band radar that flew onboard the Space Shuttle Endeavour during an 11-day mission in February of 2000. The surface elevation from InSAR at vegetated areas are elevation of the "scattering center" within the canopy (Sarabandi & Lin, 2000). The SRTM elevation data from the C-band InSAR data at one-arc second resolution

[1] Renamed as National Geospatial-Intelligence Agency — NGA since Nov. 2003.

(nominally 30 m) (http://edc.usgs.gov/products/elevation.html) were used in this study to verify the location accuracy of GLAS data, and make a comparison with the elevation derived from GLAS data.

3. Data processing method

3.1. GLAS data processing

The GLA14 data were searched, and all shots in the study area were retrieved along with the record index, the serial number of the shot within the index (from 1 to 40), acquisition time, latitude, longitude, elevation, range offsets of signal beginning, signal ending, waveform centroid, and fitted Gaussian peaks. Since the elevation in GLA14 is referenced to TOPEX/Poseidon ellipsoids and is the height of the waveform centroid, it has to be converted into ground surface height (the last Gaussian peak, i.e. ground peak) and referenced to the WGS84 geoid used for SRTM DEM data. The offset difference between signal beginning and end is defined as waveform length (wflen), and the distance between the signal beginning and the last Gaussian peak is defined as the top tree height.

In the GLA01 data file, the 40 shots received in 1 s are assigned only one estimated latitude and longitude. Using the record index and shot number found in GLA14 data, the individual waveform was extracted from GLA01 data along with other parameters such as estimated noise level, noise standard deviation, and transmitted pulse waveform, which were used later in waveform processing.

The location accuracy of the GLAS footprints was evaluated by matching the elevation profile from GLAS with the existing SRTM DEM. GLAS data transects acquired over a 15-second period (600 footprints) were used. The one-arc-second SRTM data were re-sampled into 10 m and 60 m pixel sizes. The geolocation of GLAS footprint was used to find the corresponding pixel in SRTM data. For 60 m pixel SRTM data, the elevation of this pixel was used. For SRTM data re-sampled into 10 m pixel, a 7 by 7 window centered on the pixel was used to get mean elevation for the GLAS footprint. The correlation between SRTM DEM and the elevation from GLAS at the footprint locations were calculated. The maximum correlation between GLAS elevation and SRTM elevation transects was found by moving the GLAS footprint transect in north–south and east–west directions within the SRTM DEM images and re-calculating the correlations. The elevation differences between SRTM and GLAS elevations were also calculated. The calculated differences are the heights of the "scattering center" which are often used in the InSAR literature, and are indicators of the canopy structure (Sarabandi & Lin, 2000).

A method for calculating the heights of quartile waveform energy from GLAS waveform was developed. The waveform was first filtered by a Gaussian filter of a width similar to the transmitted laser pulse. In Fig. 5, the points represent the waveform, and the solid curve along the points represents the smoothed waveform. The GLA01 product gives the estimated noise level, i.e. the mean and standard deviation of background noise values in the waveform. For many cases, the noise level before the signal beginning was lower than the noise after the signal ending. Consequently, we estimated the noise levels before the signal beginning and after the signal ending from the original waveform separately using a method based on the histogram. For example, the histogram of the waveform bins from the signal beginning to the last bin (544) (the top part of the waveform in Fig. 5) was generated, and its peak was fitted with a Gaussian curve. The peak of the curve was used as the noise level. The standard deviation of the noise was, then calculated from these waveform bins. The vertical lines along the noise levels at both ends of the waveform are the estimated noise levels (Fig. 5).

Using three standard deviations as a threshold above the noise level, the signal beginning and ending were located. The total waveform energy was calculated by summing all the return energy from signal beginning to ending. Starting from the signal ending, the position of the 25%, 50%, and 75% of energy were located by comparing the accumulated energy with total energy. Since the heights of these quartiles refer to the ground surface, not the signal ending, the ground peak in the waveform needs to be located. Searching backward from the signal ending, the peaks can be found by comparing a bin's value with those of the two neighboring bins. If the first peak is too close to the signal ending, i.e. the distance from signal ending to the peak is less than the half width of the transmitted laser pulse, this peak was discarded. The first significant peak found is the ground peak. The tree height of 33.43 m in Fig. 5 was the distance from signal beginning to the ground peak, and is equal to H100. As terrain slope and surface roughness increase, the ground peak of the

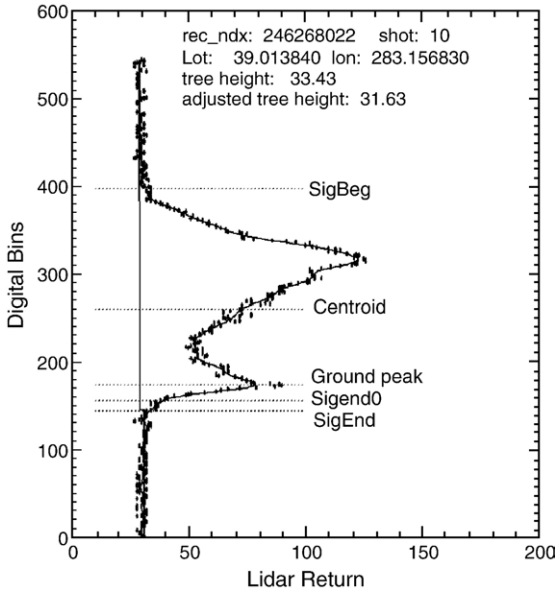

Fig. 5. Processing of a GLAS waveform: Waveform (dots) was first smoothed by a filter. The noise mean and standard deviation was estimated separately for tails at the two ends, from which thresholds were set and used to locate the signal beginning and end. The ground peak was searched from the signal end upwards. Waveform energy centroid (50%) and other energy quartiles can be calculated. For a smooth flat surface, the distance between signal end and ground peak should be the same as the half width of transmitted pulse (from SigEnd0 to ground peak). Surface slope widened the ground peak from SigEnd0 to SigEnd.

waveform becomes wider and the signal beginning moves upwards in a proportional manner. The dashed line between the ground peak and signal ending is the assumed signal ending (SigEnd0) if there is no widening of the ground peak. The distance between the signal ending and the assumed signal ending was used as an adjustment to the signal beginning. The height of 31.63 m in Fig. 5 is the adjusted tree top height, and is referred to as Ht. In addition, the method for estimation of canopy height profile from lidar waveform described by Lefsky et al. (1999b) was used to calculate the mean, median, and quadratic mean heights of the canopy.

3.2. Extracting LVIS data

In the enlarged box in Fig. 2, the pixel size of the background image is 15 m, and the yellow circles indicate the location of LVIS shots. The nominal diameter of the LVIS shot is 20 m. Therefore the LVIS shots were dense enough to provide maps of the canopy vertical structure. A 60 m circle shown in the figure includes about 40 LVIS shots. For this study, the LVIS shot data was used without rasterization. All LVIS shots within circles with 60 m and 120 m diameters centered at each GLAS footprint were extracted from the LVIS lge data, and the statistics of the quartile heights (H25, H50, H75, and H100) were calculated. The height indices derived from GLAS waveform and LVIS data were compared. The linear correlation of two vectors was used to evaluate their relationship. Within the area where the LVIS waveforms are available, all LVIS waveforms within the 60 m or 120 m circles centered at GLAS footprints were extracted and added together by aligning them with waveform ground peaks or the surface heights. The aggregated LVIS waveforms were compared with the GLAS waveforms.

Neter and Wasserman (1974)described how to use *F*-test to test whether two regression lines identical, and use *t*-test to make comparisons of regression parameters such as the slopes. The *F*-test includes following steps: 1) fit the full model (two independent regression models) and obtain the error sum of squares SSE(F); 2) obtain the reduced model (with hypothesis that these two regression lines are the same, i.e. one regression model using combined data) and determine SSE(R); 3) calculate the F^* statistic. Large values of F^* lead to the negative of the hypothesis, that the slope or intercept or both are different between the two regressions. The comparison of slopes from two regression lines was conducted by constructing an interval

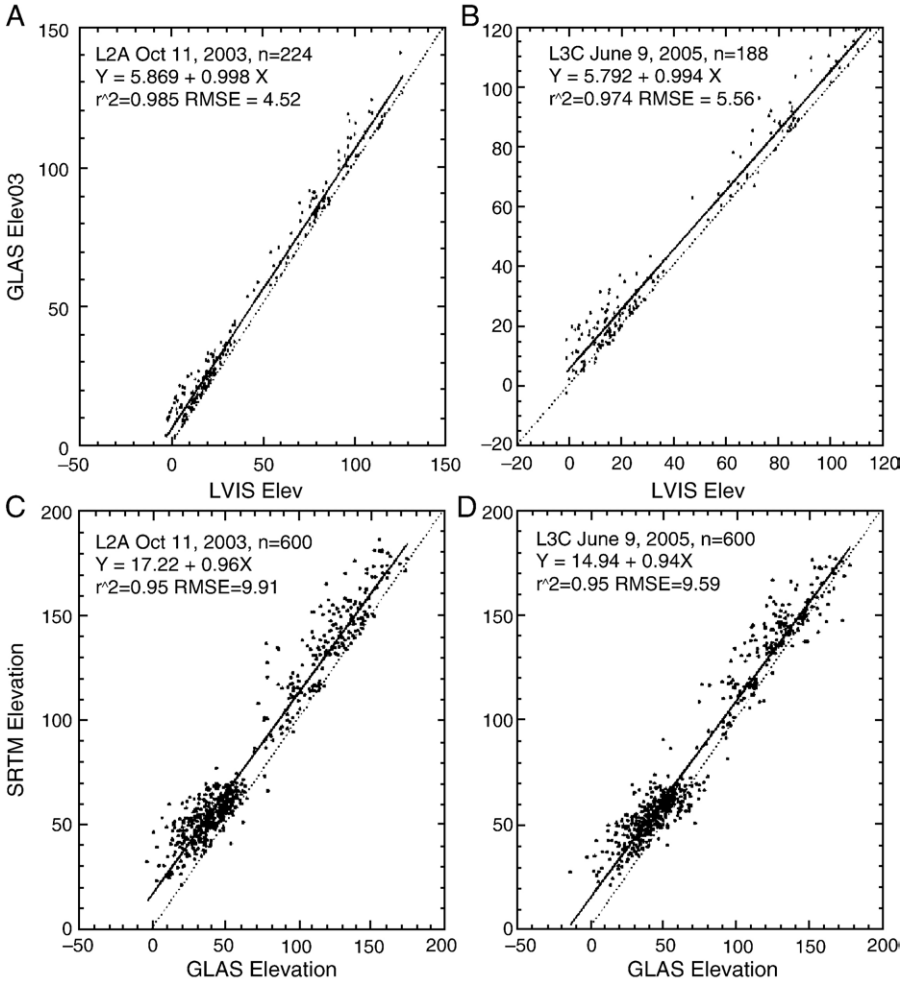

Fig. 6. Comparisons of surface elevations from LVIS and GLAS (all axes are in meters): A — LVIS Elevation and GLAS Elevation along Oct 11, 2003 GLAS footprints; B — LVIS Elevation and GLAS Elevation along June 9, 2005 GLAS footprints; C and D — Surface elevations from GLAS and SRTM DEM. Dotted lines in all figures are 1:1 lines.

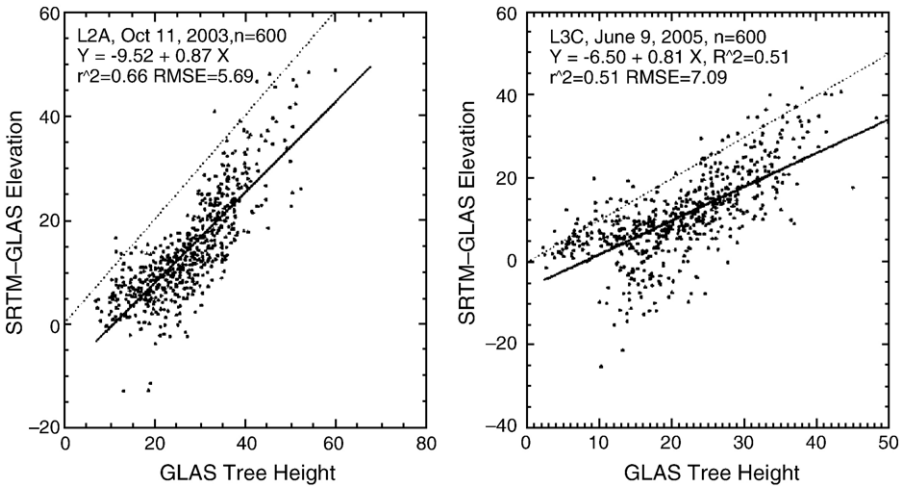

Fig. 7. Scatter plots of tree height measured by GLAS (H14) and the height of SRTM scattering phase center. Solid lines are the best linear fit to the data, and dotted lines are 1:1 lines. Test statistic showed that the slopes of these two regression lines were not significantly different at 95% confidence level, but the regression equations are significantly different. This indicates that the intercepts of these regression lines are significantly different.

estimate using *t*-distribution. These tests were used in this study to compare regression relations derived from different datasets.

3.3. Seasonal effect on GLAS data

The GLAS data of Oct 11, 2003 and June 9, 2005 were nearly repeat passes, but the distances between corresponding footprints ranged from a few tens of meters to a few hundreds of meters. The 40 footprints starting from the north edge of GSFC and heading towards the northwest pass through BARC forests, agricultural fields, and roads. The distances between corresponding 2003 and 2005 footprints ranged from 38.7 m to 73.1 m. Therefore the footprints from this part of these two orbits partially overlap. The tree height indices from GLAS data were compared to assess any temporal differences between the two GLAS overpasses.

4. Results and discussion

4.1. Location accuracy of GLAS footprints

For the data acquired on Oct. 11, 2003, the correlation between 60 m SRTM DEM and GLAS elevations was $r^2 = 0.986$. Shifting the GLAS transect westwards by one pixel in column direction resulted in the maximum correlation of $r^2 = 0.992$. For the GLAS data acquired on June 9, 2005, the same shift increased the correlation coefficient from 0.982 to a maximum of 0.992. For the SRTM DEM data with 10 m pixel size, the same correlation analysis found that the maximum correlation was 0.895 for both GLAS dates, and a (−2,1) pixel shifting was needed. These results show that the GLAS footprint location error is small, as described by Carabajal and Harding (2005).

4.2. Elevation from GLAS

The comparisons of surface elevations from GLAS and LVIS in Fig. 6A and B show that the GLAS surface heights acquired on Oct 11, 2003 and June 9, 2005 were consistent. A *F*-test showed that at 95% confidence level there was no significant difference between these two regression lines in Fig. 6A and B. The intercepts in Fig. 6A and B show that the elevations from GLAS and LVIS have a systematic bias. The elevation from GLAS was higher than that from LVIS. The LVIS elevation here was an average of several tens of LVIS shots within a GLAS footprint. The causes of this bias needs further study, but the consistence of these two orbits indicates the stable performance of these lidar systems.

Fig. 6C and D show the comparisons of elevations from SRTM and the nearly repeat passes of GLAS orbits on Oct 11, 2003 and June 9, 2005. The plots in Fig. 6C and D show GLAS footprints acquired over a 15-second period. The SRTM elevation is the height of the radar scattering center of the targets, and the GLAS elevation is the height of the ground surface. Both are referenced to the WGS84 geoid. A *t*-test showed that at 95% confidence level there was no significant

Table 1
Correlations (r^2) between the tree height indices derived from GLAS waveforms and averaged LVIS data within the GLAS footprint

LVIS	Height indices derived from GLAS data								
	MedH	MeanH	QMCH	wflen	H14	H25	H50	H75	H100
10/11/03									
H25	0.68	0.66	0.68	0.58	0.42	**0.54**	0.77	0.82	0.62
H50	0.69	0.69	0.71	0.61	0.45	0.52	**0.77**	0.83	0.65
H75	0.67	0.68	0.71	0.63	0.48	0.48	0.73	**0.82**	0.66
H100	0.65	0.66	0.69	0.64	0.49	0.69	0.48	0.79	**0.66**
06/09/05									
H25	0.50	0.54	0.55	0.55	0.32	**0.60**	0.66	0.63	0.54
H50	0.53	0.58	0.59	0.59	0.35	0.59	**0.66**	0.65	0.58
H75	0.53	0.58	0.59	0.61	0.38	0.56	0.65	**0.65**	0.60
H100	0.52	0.58	0.69	0.64	0.40	0.54	0.64	0.64	**0.62**

Bolded numbers are correlations between the same quartile energy heights from LVIS and GLAS.

difference between the slopes of these two regression lines in Fig. 6C and D. But an *F*-test showed that these two regression equations were significantly different at the same confidence level due to the different intercepts. The elevation differences were larger on Oct 11, 2003 than on June 9, 2005. This difference was mainly due to that the elevation from SRTM is the height of scattering center within forest canopy. Other factors, such as the noise of SRTM InSAR data, the error of GLAS elevation, contribute to this difference too.

The correlation between the heights of the scattering center, i.e. the elevation difference between SRTM and GLAS DEM and the tree height measured from GLAS is significant as shown in Fig. 7. This is consistent with findings from our previous studies (Sun et al., 2003). Because the height of the scattering center (SRTM-GLAS) should be greater than zero, and less than the actual maximum tree height, all data points should fall in the area between the 1:1 line and $y=0$ line. There are points in Fig. 7 which are below line $y=0$, especially in the case of June 9, 2005 GLAS data. The elevation in GLA14 was referred to a point called "Land range offset" (D. Harding, personal communication). For a bare surface, this location should be the ground surface. If the vegetation exists, it needs to be adjusted to ground surface (location of the ground peak). For some waveforms without obvious ground peaks, this causes the error in GLAS surface elevation. In both cases, the intercepts of the regression lines were not equal to zero, and the correlation between the height of the scattering center and top tree height was significant. These indicate that the height of radar scattering center is a complex function of the canopy structure including the parameter of the top tree height.

4.3. Comparisons of GLAS height indices with averaged LVIS height indices

The correlations between tree height indices derived from LVIS and GLAS are shown in Table 1 for the GLAS data of Oct

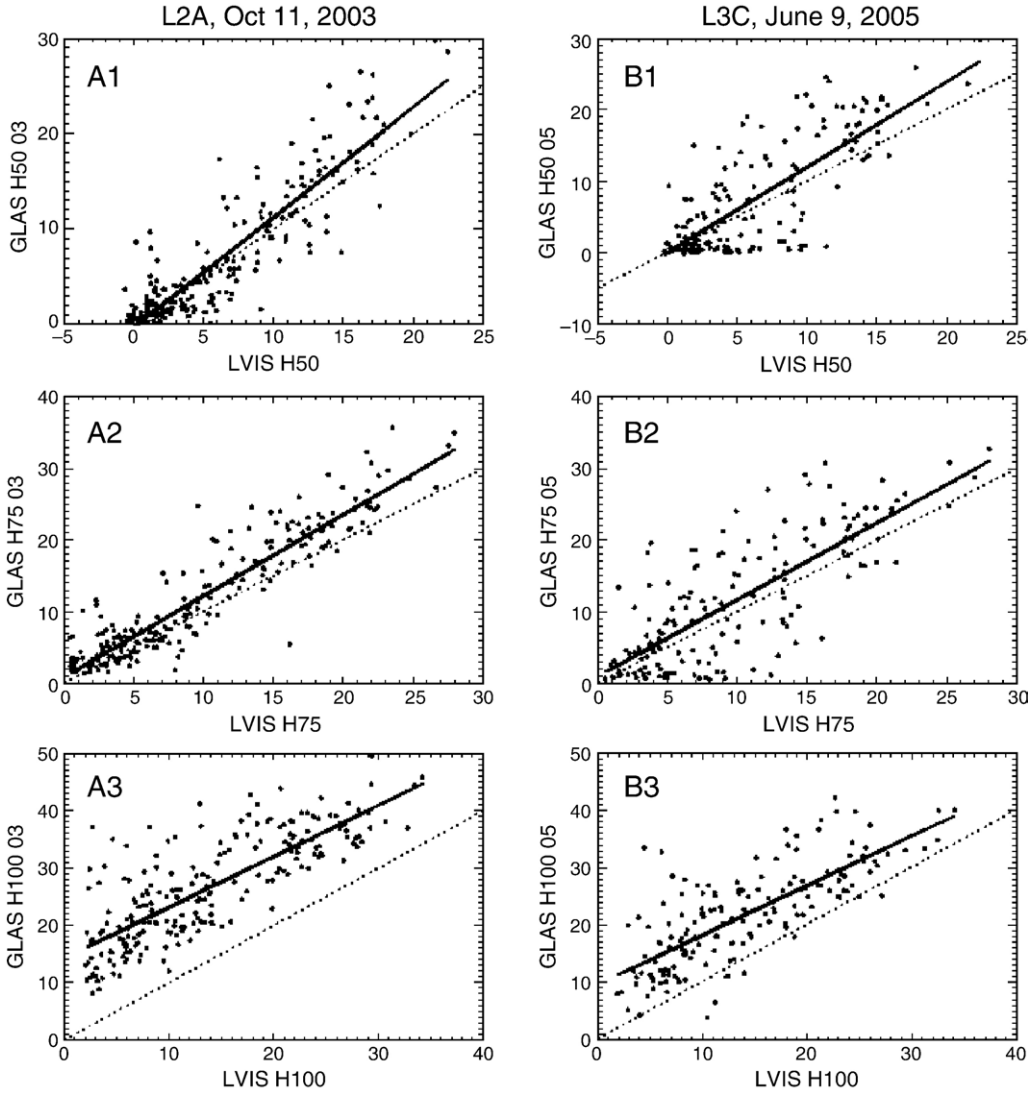

Fig. 8. Comparisons of waveform quartile heights derived from LVIS and GLAS data on Oct 11, 2003 (left column), and June 9, 2005 (right column). Statistic tests shown that the regression lines were not significantly different (at 95% confidence level) in A1 and B1, and in A2 and B2. In A3 and B3, the slopes of the two regression lines have no significant difference, but the regression lines (equations) are significantly different.

Table 2
The regression coefficients and Root-Mean-Square-Error: $H_{xx}^{GLAS}=A_0+A_1H_{xx}^{LVIS}$, where xx=50, 75 and 100

GLAS	A_0	A_1	r^2	RMSE	*t*-test	*F*-test
H50 2003	−0.311	1.450	0.806	3.10	−0.02053	−18.57
H50 2005	0.051	1.189	0.613	4.82		
H75 2003	0.845	1.137	0.861	3.15	0.04447	−18.45
H75 2005	0.954	1.073	0.615	5.42		
H100 2003	14.230	0.888	0.633	5.52	−0.0244	**4.652**
H100 2005	9.600	0.867	0.580	5.55		

t-tests were used to test the difference in regression slopes, and *F*-tests were used to test the difference in regression equations. The results show that the only significant difference is between two regression equations for H100 (*F*-test statistics is bolded), and all others have no significant differences at 95% confidence level.

11, 2003 and June 9, 2005. It can be seen that the linear correlation coefficient (r^2) between the averaged LVIS indices and indices derived from the GLAS waveforms is significant for most cases. For both dates, the correlations between averaged LVIS quartile heights and GLAS quartile heights are high. For the GLAS data acquired on Oct 11, 2003, the GLAS H75 has the highest correlations with the average quartile heights H50 (r^2=0.83) and H75 (r^2=0.82) from LVIS data. The quartile height H50 from LVIS data, also called as height of mean energy (HOME) of waveform, was found to be highly correlated with forest biomass (Drake et al., 2002). Therefore, because of their higher correlation with LVIS H50, the GLAS H50 and H75 should be good indication of forest biomass.

Generally the correlations were higher for the GLAS data acquired on Oct 11, 2003 than for the data acquired on June 9, 2005. Fig. 8 shows the comparisons of waveform quartile heights derived from LVIS and GLAS data on Oct 11, 2003 (left column), and June 9, 2005 (right column). The correlation equations, r^2, and root-mean-square-error are listed in Table 2. The *t*-test and *F*-test were used to test if the regression equations (lines) for 2003 and 2005 GLAS data are significantly different at 95% confidence level. The results (*F*-test in Table 2) show that the regression lines were not significantly different between A1 and B1, and between A2 and B2. In the case of A3 and B3, the slopes of the two regression lines have no significant difference (*t*-test), but the regression lines (equations) are significantly different from the *F*-test. Because of smaller footprint sizes, LVIS should be more sensitive to the top of the canopy, and give the spatial structure of canopies in more detail. The results show that the H50 and H75 are less sensitive to the lidar footprint size.

4.4. GLAS waveform and aggregated LVIS waveform

In order to further check the information content, especially the vertical structure of the GLAS data, the waveforms of the two GLAS footprints shown in Fig. 2 were compared with the simulated waveform by aggregating LVIS waveforms within the footprints. We used the location of the GLAS footprint, and extracted all LVIS waveforms within a 60 m and 120 m diameter circle. Although the laser pulse power within the footprint is a Gaussian distribution, for simplicity we assumed that the laser pulse power within the footprint was constant. One aggregation was made by aligning all LVIS waveforms by their ground peaks of the waveforms without considering the elevations of these peaks. The other aligned the waveforms by their laser ranges. The local ground surface slopes of these two footprints were small (3.4 and 4.5°). All simulated waveforms were similar to the corresponding GLAS waveforms. The aggregated LVIS waveforms aligned by laser ranges in a 60 m-diameter circle most closely resemble the GLAS waveforms. Fig. 9 shows the comparisons for these two GLAS waveforms. The vertical distances of waveform digital bins are 30 cm (2 ns) and 15 cm (1 ns) for LVIS and GLAS, respectively. The comparisons show

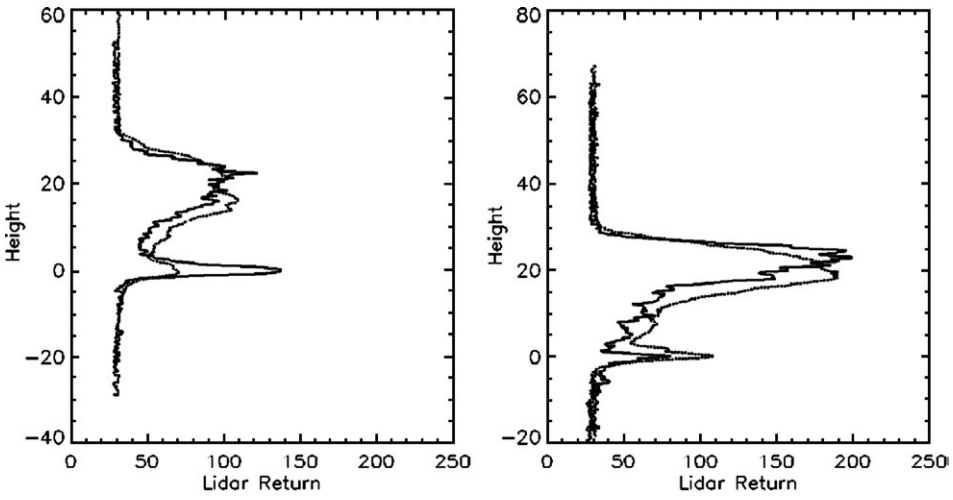

Fig. 9. LVIS waveforms within a 60 m circle were aggregated to simulate the GLAS waveform. The LVIS waveforms were aligned by laser ranges. The dotted lines are the aggregated LVIS waveforms. Solid curves are GLAS waveforms. Left figure shows the GLAS waveform from shot 246268022-6, acquired on Oct. 11, 2003. Right figure shows the GLAS waveform from shot 770884762-1, acquired on June 9, 2005.

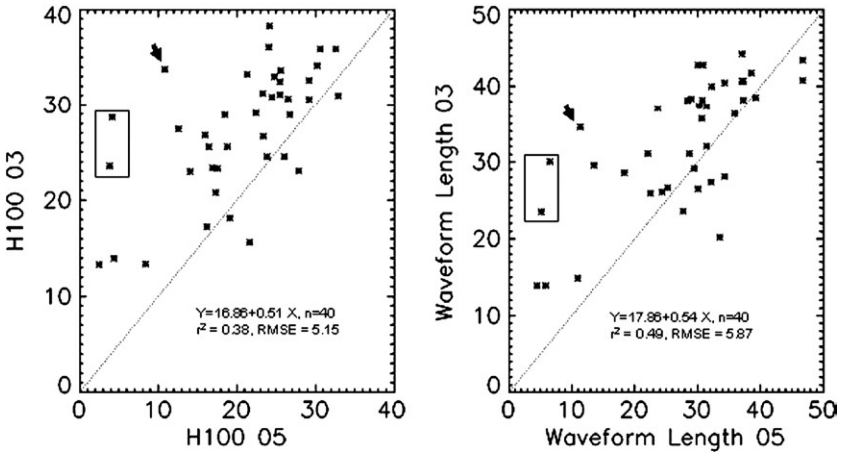

Fig. 10. Comparisons of tree height measured by GLAS on Oct 11, 2003 and June 9, 2005. The GLAS footprints from 246268012-37 to 246268022-37 acquired by Laser 2 (L2A) on Oct. 11, 2003, and footprints from 770884752-32 to 770884762-32 acquired by Laser 3 (L3C) were nearly repeat passes over the study area. Left figure shows the top tree height, and the right figure shows the total vertical length of waveform. The two outliers in the box were along a forest edge and the other outlier indicated by arrow was near a road.

that the vertical information in the scale of the GLAS footprint is similar for GLAS and LVIS data.

4.5. Seasonal changes and forest heterogeneity

We have shown that the surface elevation measured by GLAS on Oct. 11, 2003 and June 9, 2005 were consistent (Fig. 7), and that the quartile heights H50 and H75 derived from GLAS waveform from the two dates were highly correlated with LVIS data without significant differences. But the correlations for H100 between GLAS and LVIS are significantly different (Table 2) due to the different intercepts. Fig. 10 shows the comparisons of the top tree height and the total length of waveform (from signal beginning to end) measured by GLAS on Oct 11, 2003 and June 9, 2005. Forty GLAS footprints from the north edge of GSFC to northwest were plotted in Fig. 10. These two orbits were near repeat passes. The distances between corresponding footprints range from 38.7 m to 73.1 m for these footprints. These two paths were passing forests, cornfield and roads. There are a few trees and small single-story buildings around the cornfields, and trees along the roadside. The average top tree height is 26.04 m (standard deviation 8.33 m) from GLAS L2A, and 22.95 m (7.56 m) from GLAS L3C. The average waveform length is 27.66 m (10.80 m) and 32.73 m (8.31 m), respectively. It was possible that some footprints (such as the three outliers shown in Fig. 10) from 2003 hit the trees and those from 2005 didn't. Most of the footprints were in forests, and the top tree height differences are from differences in the forest structures. Since the ground surface elevation from these two GLAS data sets was consistent, the difference in top tree height was from the difference in the signal beginning of the waveforms. This can be caused by different density of foliage, even though trees in both early October and June should have full leaf canopies. The other factor for the height differences from near-repeat pass GLAS data is the horizontal heterogeneity of the forest canopies. Further detailed studies are needed to identify the major factors.

5. Conclusions

The Geoscience Laser Altimeter System (GLAS) is the first lidar instrument for continuous global observation of the Earth. It samples the earth surface every 175 m along track with an ellipsoid footprint of about 120 m by 50 m for laser 2, and a circular footprint of about 65 m for laser 3. In this study, SRTM DEM data were used to estimate the GLAS footprint location error. The airborne Laser Vegetation Imaging Sensor (LVIS) with scanning capability was used to provide a smaller footprint and many more samples of the surface within the GLAS footprints and provided an independent check of the GLAS data.

The SRTM and GLAS elevation data comparisons provide an independent check of the geolocation accuracy of GLAS data. The results indicate that the GLAS footprint location error on the ground is less than 60 m, and probably much smaller. The surface elevation measured from GLAS and LVIS were consistent. Correlations between tree height indices derived from LVIS and GLAS were relatively high (e.g., $r^2=0.82$ for LVIS H75 and GLAS H75; and $r^2=0.83$ for LVIS H50 and GLAS H75). In addition, the aggregated LVIS waveforms compared well with the corresponding GLAS waveforms, which indicate that the vertical information in GLAS and LVIS waveforms were similar on the scale of GLAS footprint size.

It is difficult to quantify the degree that the footprints from GLAS and LVIS cover the exact same canopy. Nevertheless, this study shows that the tree height indices from both instruments are highly correlated and give reasonable measurements of canopy vertical structure. The quartile waveform energy heights H50 and H75 derived from GLAS and LVIS data showed higher correlations than H100. Because of these high correlations and the fact that airborne lidar data has been shown to be an accurate index of forest biomass, we believe that the GLAS data will be useful for biomass sampling in regional to global scales. However, caution and further study should be taken in terms of the effects of seasons of data acquisition, the

scale of the sample as well as terrain slope and forest types on the derived forest structure measures.

Acknowledgement

This study was funded by NASA's Science Mission Directorate. The LVIS data sets were provided by the Laser Vegetation Imaging Sensor (LVIS) team in the Laser Remote Sensing Branch at NASA Goddard Space Flight Center with support from the University of Maryland, College Park. Funding for the collection and processing of the northeastern USA data was provided by NASA's Terrestrial Ecology Program (NASA Grant number NAG512112).

References

Abshire, J. B., Sun, X., Riris, H., Sirota, J. M., McGarry, J. F., Palm, S., et al. (2005). Geoscience Laser Altimeter System (GLAS) on the ICESat mission: On-orbit measurement performance. *Geophysical Research Letters*, *32*(22).

Blair, J. B., Hofton, M. A., & Rabine, D. L. (2004). *Processing of NASA LVIS elevation and canopy (LGE, LCE and LGW) data products, version 1.0.* https://lvis.gsfc.nasa.gov

Blair, J. B., Rabine, D. L., & Hofton, M. A. (1999). The laser vegetation imaging sensor (LVIS): A medium-altitude, digitations-only, airborne laser altimeter for mapping vegetation and topography. *ISPRS Journal of Photogrammetry and Remote Sensing*, *54*, 115−122.

Carabajal, C. C., & Harding, D. J. (2005). ICESat validation of SRTM C-band digital elevation models. *Geophysical Research Letters*, *33*, L22S01.

Drake, J. B., Dubayah, R. O., Clark, D. B., Knox, R. G., Blair, J. B., Hofton, M. A., et al. (2002). Estimation of tropical forest structural characteristics using large-footprint lidar. *Remote Sensing of Environment*, *79*, 305−319.

Drake, J. B., Knox, R. G., Dubayah, R. O., Clark, D. B., Condit, R., Blair, J. B., et al. (2003). Above-ground biomass estimation in closed canopy neotropical forests using lidar remote sensing: Factors affecting the generality of relationships. *Global Ecology and Biogeography*, *12*(2), 147−159.

Dubayah, R. O., & Drake, J. B. (2000). Lidar remote sensing for forestry. *Journal of Forestry*, *98*(6), 44−46.

Harding, D. J., & Carabajal, C. C. (2005). ICESat waveform measurements of within-footprint topographic relief and vegetation vertical structure. *Geophysical Research Letters*, *32*. L21S10. doi:10.1029/2005GL023471.

Harding, D. J., Lefsky, M. A., Parker, G. G., & Blair, J. B. (2001). Laser altimeter canopy height profiles — Methods and validation for closed-canopy, broadleaf forests. *Remote Sensing of Environment*, *76*(3), 283−297.

Hese, S., Lucht, W., Schmullius, C., Barnsley, M., Dubayah, R., Knorr, D., et al. (2005). Global biomass mapping for an improved understanding of the CO_2 balance — The Earth observation mission Carbon-3D. *Remote Sensing of Environment*, *94*(1), 94−104.

Hofton, M. A., Minster, J. B., & Blair, J. B. (2000). Decomposition of laser altimeter waveforms.*IEEE Transactions on Geoscience and Remote Sensing*, *38*(4), 1989−1996 (Part 2).

Hurtt, G. C., Dubayah, R., Drake, J., Moorcroft, P. R., Pacala, S. W., Blair, J. B., et al. (2004). Beyond potential vegetation: Combining lidar data and a height-structured model for carbon studies. *Ecological Applications*, *14*(3), 873−883.

Hyde, P., Dubayah, R., Peterson, B., Blair, J. B., Hofton, M., Hunsaker, C., et al. (2005). Mapping forest structure for wildlife habitat analysis using waveform lidar: Validation of montane ecosystems. *Remote Sensing of Environment*, *96*(3-4), 427−437.

Lefsky, M. A., Cohen, W. B., Acker, S. A., Parker, G. G., Spies, T. A., & Harding, D. (1999a). Lidar remote sensing of the canopy structure and biophysical properties of Douglas-fir western hemlock forests. *Remote Sensing of Environment*, *70*(3), 339−361.

Lefsky, M. A., Cohen, W. B., Harding, D. J., Parker, G. G., Acker, S. A., & Gower, S. T. (2002). Lidar remote sensing of above-ground biomass in three biomes. *Global Ecology and Biogeography*, *11*(5), 393−399.

Lefsky, M. A., Harding, D., Cohen, W. B., Parker, G., & Shugart, H. H. (1999b). Surface lidar remote sensing of basal area and biomass in deciduous forests of Eastern Maryland, USA. *Remote Sensing of Environment*, *67*, 83−98.

Lefsky, M. A., Harding, D. J., Keller, M., Cohen, W. B., Carabajal, C. C., Espirito-Santo, F. D., et al. (2005c). Estimates of forest canopy height and aboveground biomass using ICESat. *Geophysical Research Letters*, *32*(22).

Lefsky, M. A., Hudak, A. T., Cohen, W. B., & Acker, S. A. (2005a). Geographic variability in lidar predictions of forest stand structure in the Pacific Northwest. *Remote Sensing of Environment*, *95*(4), 532−548.

Lefsky, M. A., Turner, D. P., Guzy, M., & Cohen, W. B. (2005b). Combining lidar estimates of aboveground biomass and Landsat estimates of stand age for spatially extensive validation of modeled forest productivity. *Remote Sensing of Environment*, *95*(4), 549−558.

NASA (2004). *Earth Science Technology Plan 2004.* NP-2005-5-700-GSFC, 31p.

Neter, J., & Wasserman, W. (1974). *Applied linear statistical models: Regression, analysis of variance, and experimental designs.* Homewood, Illinois: Richard D. Irwin, Inc.

Ranson, K. J., Sun, G., Kovacs, K., & Kharuk, V. I. (2004a). Landcover attributes from ICESat GLAs data in central Siberia. *IGARSS 2004 Proceedings, 20–24 September 2004, Anchorage, Alaska, USA*.

Ranson, K. J., Sun, G., Kovacs, K., & Kharuk, V. I. (2004b). Use of ICESat GLAS data for forest disturbance studies in central Siberia. *IGARSS 2004 Proceedings, 20–24 September 2004, Anchorage, Alaska, USA*.

Sarabandi, K., & Lin, Y. C. (2000). Simulation of interferometric SAR response for characterizing the scattering phase center statistics of forest canopies. *IEEE Transactions on Geoscience and Remote Sensing*, *38*(1), 115−125.

Schutz, B. E., Zwally, H. J., Shuman, C. A., Hancock, D., & DiMarzio, J. P. (2005). Overview of the ICESat Mission. *Geophysical Research Letters*, *32*(22).

Sun, G., Ranson, K. J., Kharuk, V. I., & Kovacs, K. (2003). Validation of surface height from shuttle radar topography mission using shuttle laser altimeter. *Remote Sensing of Environment*, *88*, 401−411.

van Zyl, J. J. (2001). The Shuttle Radar Topography Mission (SRTM): A breakthrough in remote sensing of topography. *Acta Astronautica*, *48*(5-12), 559−565.

Weishampel, J. F., Blair, J. B., Knox, R. G., Dubayah, R., & Clark, D. B. (2000). Volumetric lidar return patterns from an old-growth tropical rainforest canopy. *International Journal Of Remote Sensing*, *21*(2), 409−415.

Zwally, H. J., Schutz, B., Abdalati, W., Abshire, J., Bentley, C., Brenner, A., et al. (2002). ICESat's laser measurements of polar ice, atmosphere, ocean, and land. *Journal of Geodynamics*, *34*(3-4), 405−445.